Surface atmospheric electric field variability at a desert site

Nicoll, K. A. ORCID: https://orcid.org/0000-0001-5580-6325, Readle, A., Al Kamali, A. and Harrison, R. G. ORCID: https://orcid.org/0000-0003-0693-347X (2022) Surface atmospheric electric field variability at a desert site. Journal of Atmospheric and Solar-Terrestrial Physics, 241. 105977. ISSN 1364-6826 doi: 10.1016/j.jastp.2022.105977 Available at https://centaur.reading.ac.uk/108478/

Journal of Atmospheric and Solar–Terrestrial Physics 241 (2022) 105977

Contents lists available at ScienceDirect

Journal of Atmospheric and Solar-Terrestrial Physics

journal homepage: www.elsevier.com/locate/jastp

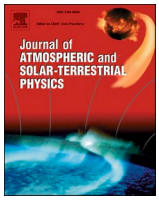

Research Paper

Surface atmospheric electric field variability at a desert site

K.A. Nicoll [a,*], A. Readle [a,b], A. Al Kamali [a,c], R.G. Harrison [a]

[a] Department of Meteorology, University of Reading, UK
[b] Met Office, Exeter, UK
[c] Department of Research, Development and Training, National Center of Meteorology, Abu Dhabi, United Arab Emirates

ARTICLE INFO

Keywords:
Potential gradient
United Arab Emirates
Sea breeze
Convection
Dust electrification

ABSTRACT

Measurements of atmospheric electrical variables in arid desert environments provide a route to assessing dust charging, which affects dust lofting; satellite remote sensing of dust particles; long range transport of elevated dust layers; and may also influence rain droplet size. This paper analyses a new dataset of atmospheric electric field (or Potential Gradient, PG) measurements from an arid site, at Al Ain in the United Arab Emirates (UAE), to investigate the influence of local meteorological and dust processes on the PG, and assess whether global atmospheric electric signals are detectable. With no data selection applied, the diurnal PG variation has a single maximum around 14UT (18LT), which is likely to be associated with the sea breeze, present on 77% of days in the central UAE. Despite the abundance of apparently fine days meteorologically, conventional atmospheric electricity fair weather selection criteria are not effective at removing all locally generated PG variability. Even applying much stricter selection criteria (10 m wind speed(U_{10})between 1 and 5 m/s, visual range >25 km, and no present weather), a diurnal variation in PG with a single maximum at 07UT (11LT) remains, likely due to local convection at sunrise. Although the stricter criteria can remove the sea breeze effect – associated with a visual range change - the PG measurements remain dominated by local meteorological and dust processes. This obscures the usual behaviour of the Global Electric Circuit. Exceptionally large PG values (~kV/m, even for $U_{10} < 8$ m/s when no dust events are detectable visually) indicate that such desert regions can be a highly electrified environment, at least during daytime and during the summer convective months. The regular generation of highly charged dust observed is relevant to evaluating charge effects on large range transport of dust, preferential scavenging of charged dust by water droplets and obtaining accurate satellite retrievals of dust concentration.

1. Introduction

Atmospheric electricity measurements in desert regions, and notably the Potential Gradient,[1] have revealed the importance of dust in defining the local atmospheric electrical environment (e.g. Harris, 1967; Kamra, 1972; Williams et al., 2009; Yair et al., 2016; Katz et al., 2018; Nicoll et al., 2020). PG measurements are now made in an increasing number of locations world-wide (e.g. Nicoll et al., 2019), but measurements in arid, desert environments such as the Mitzpe-Ramon site in Israel (Yaniv et al., 2016) remain rare. PG values in dusty arid conditions can exceed ±10 kV/m, in comparison to typical mid-latitude fair weather PG values of ~100 V/m. Such large PG values are often associated with dust lofting processes, where, when the wind speed exceeds a threshold value (e.g. Kurosaki and Mikami, 2007), particles are suspended above the surface by the wind, and collide with each other, transferring their charge between them (Zheng, 2013). The PG is often highly variable in the presence of charged dust and can be positive or negative, thought to be related to the dust mineral composition (e.g. Kamra, 1972), as well as vertical charge structures that may arise through gravitational settling or dynamical mixing processes (Rudge, 1913; Zhang and Zhou, 2020). Previous work also demonstrates close links between the magnitude of the PG changes during dust episodes and the wind speed (e.g. Nicoll et al., 2020), and the number concentration of dust particles (Esposito et al., 2016). A detailed review of electrification processes in dust is given by Zheng (2013).

Assessing the prevalence of dust particle electrification has wide applications, because of effects on the properties of insulators on transmission lines (Awad et al., 2002), attenuation of electromagnetic wave propagation used in satellite remote sensing of dust particles (Zhou et al., 2005), effects on the orientation of dust particles (also

* Corresponding author.
E-mail address: k.a.nicoll@reading.ac.uk (K.A. Nicoll).

[1] The potential gradient PG and the vertical electric field component E are related by PG = -E.

https://doi.org/10.1016/j.jastp.2022.105977
Received 27 June 2022; Received in revised form 6 October 2022; Accepted 17 October 2022
Available online 21 October 2022

influencing radiative transfer through dust layers) (Ulanowski et al., 2007), and influencing the long range transport of elevated dust layers (van der Does et al., 2018).

Away from dusty regions, Earth's atmospheric fair weather electric field has been known about since the time of Benjamin Franklin. It results from the action of Global Electric Circuit (GEC, Wilson, 1921). The GEC framework balances large scale current flow around the planet, with charge separated vertically inside thunderstorms, and transferred upwards into the upper conductive regions, and downwards to the surface by lightning, point discharge and charged precipitation (Rycroft et al., 2008). Circumstances of minimal locally generated charge are known as fair weather conditions. The ocean air PG measurements of the research vessel Carnegie are perhaps the most important piece of evidence in support of the GEC (e.g. Harrison 2013, 2020), demonstrating the same diurnal variation in PG regardless of location on the planet. The standard "Carnegie curve" diurnal variation in PG shows a minimum at around 03UT, with a single maximum at 19UT which corresponds very closely with the diurnal variation in global thunderstorm and shower cloud area (Whipple, 1929; Whipple and Scrase, 1936). The Carnegie curve can generally only be observed in fair weather conditions at sites with minimal local influences, or by extended averaging, but its presence has become one benchmark for identifying measurement sites that are capable of providing globally representative PG measurements (e.g. Nicoll et al., 2019).

Despite often fine weather meteorological conditions in desert areas, the large concentrations of dust and aerosol particles typically present in arid regions can influence the air conductivity, and thus modify the PG (Harris, 1967). Furthermore, the particles themselves can become charged during surface dust generation processes (Rudge 1913) (e.g through interacting with each other, causing triboelectrification), or transport processes (Nicoll et al., 2011).

In this paper we characterise the variability of the PG at 3 m measured at the arid desert site of Al Ain in the UAE. This dataset was discussed in Nicoll et al. (2020), in considering the influence of sea breeze dust lofting on the PG measurements, but here we analyse the whole dataset. The objective of the paper is to understand the influence of several meteorological process on the PG in arid regions, and also consider whether sufficiently undisturbed conditions can nevertheless still occur at such a site for GEC monitoring purposes. Section 2 of this paper describes the instrumentation and site details. Section 3.1 performs some initial exploratory data analysis of the Al Ain PG dataset, followed by investigation of general meteorological influences on the PG in section 3.2. Section 3.3 explores the effect of convective processes on the PG by analysing several case studies, and section 3.4 defines the criteria used to classify fair weather conditions. Section 4 examines diurnal variations in PG, including seasonal variations (4.2), as well as diurnal variations in meteorological parameters (4.3). Further discussion is included in section 5, and conclusions in section 6.

2. Field site and instrumentation

The dataset described in this paper was obtained at Al Ain international airport (24°15′ N, 55°37′ E), in the United Arab Emirates (UAE). Al Ain has a hot desert climate (annual rainfall average of 96 mm), and the population size of the city is substantial (800,000). Although rare at Al Ain, cloud cover exists approximately 24% of the time (Yousef et al., 2019), being more common during the winter months (Nov–Mar). During the winter period, the mostly westerly and north westerly flows bring troughs, depressions, and occasional fronts into the UAE, which can provide significant rainfall. In the summer, predominantly anticyclonic conditions occur, often with a weak easterly flow bringing winds from the Gulf of Oman, and convective rainfall can be common over the Al Hajar mountains to the east of the UAE (Branch et al., 2020; Wehbe et al., 2017). A major component of development of convective activity in the UAE is the sea breeze, forming on 77% of days annually (Eager et al., 2008). It occurs all year round, but is particularly prevalent during summer. The sea breeze is generated by temperature differences between land and sea regions, caused by differential solar heating, and normally originates from the westerly coastline of the UAE, bringing moist sea air up to 300 km inland. The sea breeze front usually arrives in the region of Al Ain (170 km from the coast) by 14–15LT (10-11UT), and is characterised by a wind direction change to the NW. The sea breeze effect on the PG at Al Ain leads to a rapid increase in PG (increasing by several kV/m in less than an hour) when the sea breeze front arrives, followed by a gradual decrease to background PG levels (Nicoll et al., 2020). Finally, the UAE region generally has very large concentrations of aerosol particles (Wehbe et al., 2021), with local sources of anthropogenic pollution from construction activity and the petroleum industry (Semeniuk et al, 2015), regular dust storms, as well as smoke transport from India (Abuelgasim and Farahat, 2020). This has a seasonal variation, with winter aerosol concentrations near the surface generally greater than in summer due to less convective mixing, with lower boundary layer heights (typically 1.5 km during winter and >3.5 km during summer) (Filioglou et al., 2020).

Instrumentation to obtain the new dataset was installed at Al Ain international airport (24°15′ N, 55°37′ E), United Arab Emirates (UAE) in February 2018. This comprised a reciprocal shutter Campbell CS110 electric field mill to measure PG, Biral SWS100 visibility sensor and Vaisala CL31 ceilometer measuring backscatter from clouds and aerosol, installed approximately 2 km from the main runway. The site location and instrumentation are shown in Fig. 1. Visibility was measured to provide an indirect measurement of aerosol and/or droplets (e.g. during fog conditions), which can influence the PG by varying the conductivity. The field mill was mounted on a 3m high mast, and measured PG in the range ±20 kV/m at 1Hz temporal resolution. A "reduction factor" is often applied to PG measurements to standardise measurements to those over a horizontal surface with no instrumentation present (see e.g. Harrison and Nicoll, 2018, Appendix A). Although the reduction factor for the apparatus in its expected configuration was determined before it was shipped to the site, the actual conditions at Al Ain were never sufficiently undisturbed to allow this to be repeated after installation. From the comparisons with the apparatus made prior to the deployment, a measured PG of 100 V m^{-1} is estimated to be within 10% of the true undisturbed value. The PG and visibility data obtained were averaged to 1 min intervals for the analysis performed here. The meteorological observations used here are from regular METAR (METeorological Aerodrome Reports) reports made at the airport (approximately every 30 min). These consist of temperature, RH, wind speed, wind direction, visual range and present weather.

3. Preliminary data analysis

3.1. Characteristics of Al Ain PG data

Fig. 2 shows the time series of all Al Ain PG data, with gaps where data was not recorded due to communication issues with the data logger (see Fig. 1). The red points demonstrate that the PG is predominantly positive at Al Ain as is usual, with negative PG values (in blue) generally only occurring during rainfall or substantial dust storm events. Out of a total of 532481 PG data points, only 5553 are negative (5%).

3.2. Dependence of PG on meteorological conditions

As mentioned in the introduction, PG is highly sensitive to variations in local meteorological conditions, including the presence of precipitation, fog, and electrified clouds. At Al Ain it is expected that the PG is also highly dependent on aerosol concentration, and therefore wind speed, as this will act to loft dust from the surface, change the conductivity and charge the dust particles.

Fig. 3(a) shows the distribution of wind speeds at the Al Ain site, with a median of 3.6 m/s and maximum values reaching up to 15 m/s. It is well known that the movement of dust particles is strongly dependent on

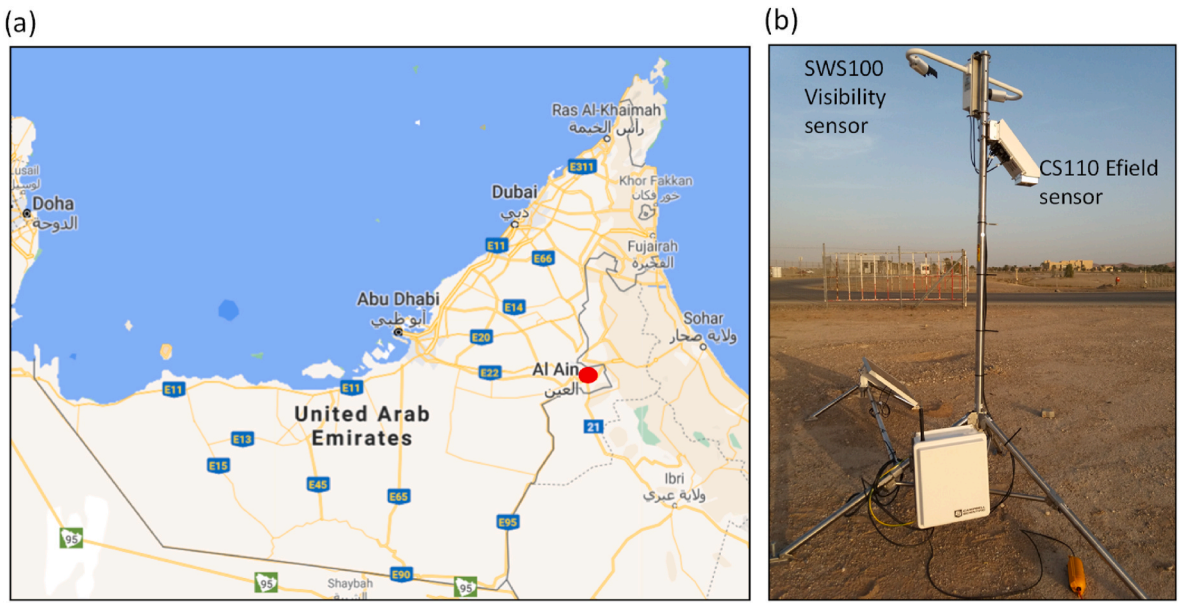

Fig. 1. (a) Map of the UAE, showing the location of the Al Ain measurement site (red dot). Image credit: Google Maps. (b) Photo of the downward-facing field CS100 Electric field mill beneath a SWS100 visibility sensor on a mast installed at Al Ain airport.

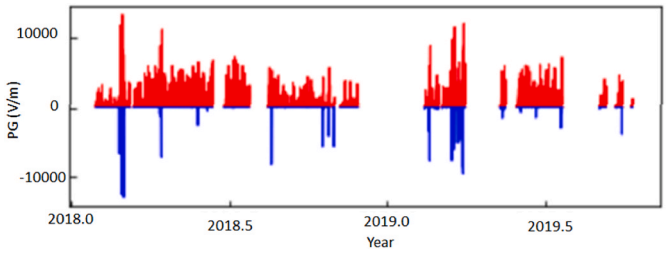

Fig. 2. Time series of PG for the two year data set at Al Ain, UAE.

wind speed, and there is a threshold wind speed above which they become lofted (e.g. Bagnold 1941; Kurosaki and Mikami 2007). Nicoll et al. (2020) established that this threshold wind speed during sea breeze events is around 6 m/s for Al Ain, above which, the magnitude of the PG increases with increasing wind speed. Such wind speeds are present approximately 20% of the time at Al Ain, therefore dust lofting is expected to be a major factor in contributing to large PG values. Reduced visibility ought to provide a robust indication of non-fair weather conditions, due to the associated presence of mist, fog, and haze (Harrison and Nicoll, 2018), but also high dust loading in desert conditions.

Fig. 3(b) shows the visibility distribution at Al Ain, where most of the values are clustered below 20 km (median = 9.8 km). The visibility distribution from non-arid sites tends to show a low visibility peak (around 1–2 km), which is associated with fog and mist conditions, but also a high visibility peak (around 40–50 km at clean air sites). The visual range sensor shows large visual ranges occasionally, but these do not dominate the visibility distribution, which is likely a result of the high concentration of dust and man-made aerosol at Al Ain, which acts to reduce the visibility on most days.

The effect of meteorological conditions on the variability of PG at Al Ain is investigated further in Fig. 4, which uses present weather codes reported from the METAR observations at Al Ain airport. Fig. 4(a) shows the variability in PG (calculated from 1 min averages) for all present weather codes in the Al Ain dataset. Present weather data is only available approximately every 30 min, hence, to provide an estimate of present weather conditions at the 1 min resolution of the PG data, the most recent present weather reading is repeated for each 30 min period until a new measurement is obtained. Conditions which involve movement of dust (i.e. blowing dust, sand storms and dust storms) produce the largest PG values (up to 4 kV/m), with large variabilities. Rainfall (which is rare) produces the largest variability in PG, but not

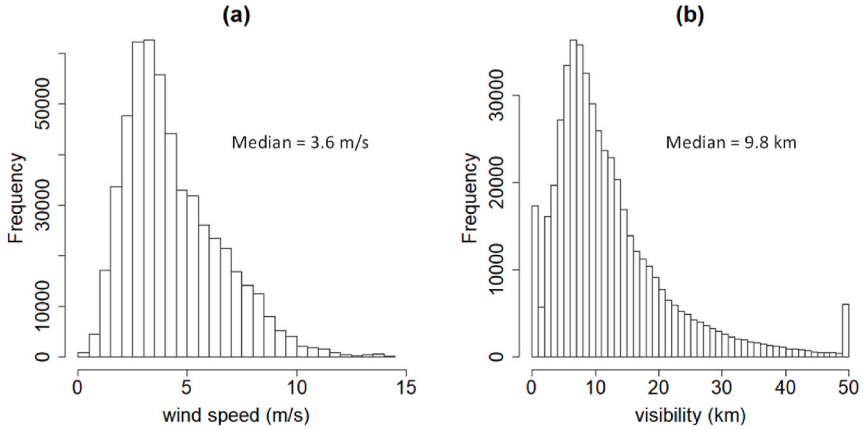

Fig. 3. (a) Distribution of 10m wind speed values at Al Ain (obtained from METAR data), and (b) visibility (as measured by the Biral SWS100 sensor).

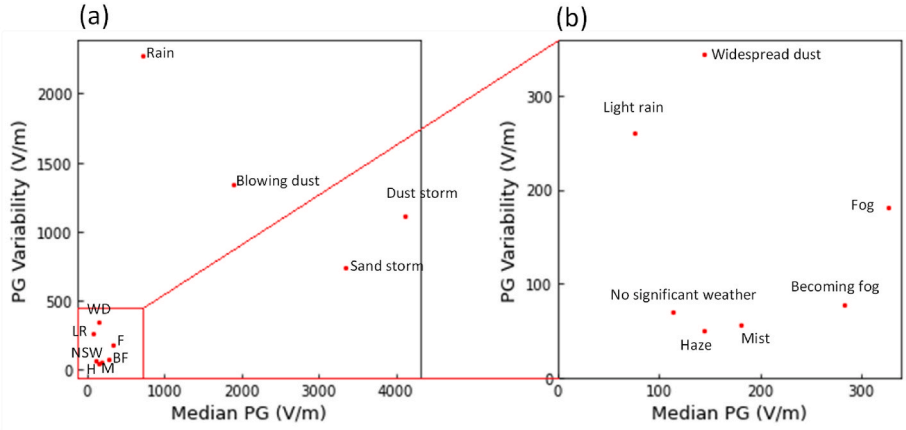

Fig. 4. Variability of PG in different types of weather conditions at Al Ain (as defined by present weather codes from the METAR observations). Variability is expressed in terms of the Inter-Quartile Range, scaled to one standard deviation for a normal distribution and calculated from 1 min averages. The y-axis IQR is ± from the median PG for each weather condition. (b) Is a close up of the red box in (a). Abbreviations inside the red box in (a) are as follows: WD = widespread dust, LR = Light rain, F = Fog, BF = Becoming fog, NSW = No significant weather, H = Haze, M = Mist.

particularly large magnitudes of PG, which is likely due to inclusion of associated negative PG values during the calculation of the median PG.

Fig. 4(b) shows a close-up image of the weather conditions included inside the red box in Fig. 4(a). These include fair weather conditions, as classified by "No significant weather" reported by the METARs. The median PG during such conditions is small (~120 V/m) compared to the other weather conditions, with low variability, as would be expected. Although the present weather code for "No significant weather" is a useful indicator of fair weather, we also employ additional criteria for our fair weather selection (as discussed in section 3.4). Finally, fog conditions are shown to produce median PG values of around 200 V/m, with low variability, as has also been observed at other sites (such as Reading, UK (Bennett and Harrison, 2007).

3.3. Investigating convective influences on PG

The hot arid climate in the UAE, with daily summer maximum temperatures often exceeding 50 °C, and winter maxima exceeding 20 °C, makes it likely that local convection will play a strong role in controlling the PG at Al Ain. This is investigated in case studies presented in Fig. 5–7.

3.3.1. PG time series

Fig. 5 (a) shows three days of PG, wind speed (at 10m) and visibility measurements during winter 2018 (31st Jan to Feb 2, 2018: year days 31–34), on dry, clear days with no cloud cover, visibility >2 km, and no significant weather reported. This is supported by the ceilometer backscatter plots in Fig. 6 which also show no cloud. These conditions would fulfil the usual criteria for fair weather (FW) days, according to Harrison and Nicoll (2018).[2] However, the PG exhibits considerable variability, particularly on days 31 and 33, with values up to 2.5 kV/m, indicating that this approach to classification would be insufficient to remove the locally generated variability. The PG on all three days shows a very similar variation to the wind speed variation, both maximising around 12UT (16LT), as would be expected for a convectively driven boundary layer (BL). The ceilometer data in Fig. 6 shows the evolution of the BL due to convection during the three days, with the BL height maximising around 11UT (15LT) on each day. The maximum wind speeds on days 31 (8 m/s) and 33 (7 m/s) exceeds the threshold wind speed for dust lofting of 6 m/s (Nicoll et al., 2020), therefore the large PG values and high variabilities on these days are likely to be associated with movement of charged dust particles. Day 32 exhibits a lower maximum wind speed (6 m/s), with maximum PG values of only ~800 V/m, supporting the conclusion that dust lofting during high wind speeds is the main cause of the large PG values on day 31 and 33. During the night, the PG is relatively stable, with small values (100–200 V/m), demonstrating that the increased PG variability during the day (particularly on days 31 and 33) is a result of convective processes driving movement of space charge and charged particles. The visibility data also provides information on the dust/aerosol content of the air, and shows a repeatable diurnal variation on days 32 and 33. The visual range is reduced (below 10 km) during the night (likely linked to higher relative humidity and trapping of aerosol at low altitudes within the BL (heights are around 800 m during the night according to Fig. 6), and increases during the day as convection acts to increase the depth of the BL to ~1500 m, mixing the particles to higher altitudes. The visibility variation on day 31 is different, however, and shows an initial decrease from 50 to 30 km in the early morning hours, followed by a recovery to 50 km. Another decrease in visibility is then observed from 10UT to 14UT, before it increases again to 40 km. The yellow values in the ceilometer data in Fig. 6(a) demonstrate that increased aerosol is present during this day, but not on days 32 and 33. This illustrates that the visibility changes, increased variability in PG, and large PG values on this day are explained by the presence of more aerosol, which becomes lofted and transported around by the relatively high wind speeds, likely generating space charge.

3.3.2. Sea breeze time series

As discussed in the introduction, Al Ain experiences regular sea breeze events, which are convectively driven, and occur all year round. Fig. 5(b) shows a time series of three days (21st-23rd March 2018: year days 80–83) of PG, wind speed and visibility data on which sea breezes occurred each day. Unlike the convective, fine days in Fig. 5(a), the daily variation in PG in Fig. 5(b) does not have a single maximum, and exhibits much more complex behaviour. The arrival of the sea breeze front is characterised by a sudden increase in PG, which takes place over an hour, followed by a slower return to lower PG values. During these periods the wind speed tends to increase, and the visibility decreases sharply. The arrival times of the sea breeze front is shown by the red arrows at the base of Fig. 5(b), and the sharp increase in ceilometer backscatter (often with a transition from blue to yellow colours), between 13UT and 16UT in Fig. 7. The PG changes during the sea breeze front passage time are largest for days 80 and 82, where the wind speeds are highest (up to 7 m/s) and increase more quickly than on day 81. The fact that the ceilometer backscatter remains increased for many hours after the sea breeze front passes, but the PG returns to smaller values, is evidence that separation of charged dust particles occurs only within the sea breeze front (Nicoll et al., 2020), and that the greater aerosol concentrations (which would reduce the conductivity), do not act to increase the PG substantially.

[2] Harrison and Nicoll (2018) defined fair weather conditions for atmospheric electricity purposes as: no hydrometeors, no aerosol or haze (i.e. visibility >2 km), no cumuliform cloud and no stratus cloud with base below 1500m, and surface wind speed between 1 and 8 m/s.

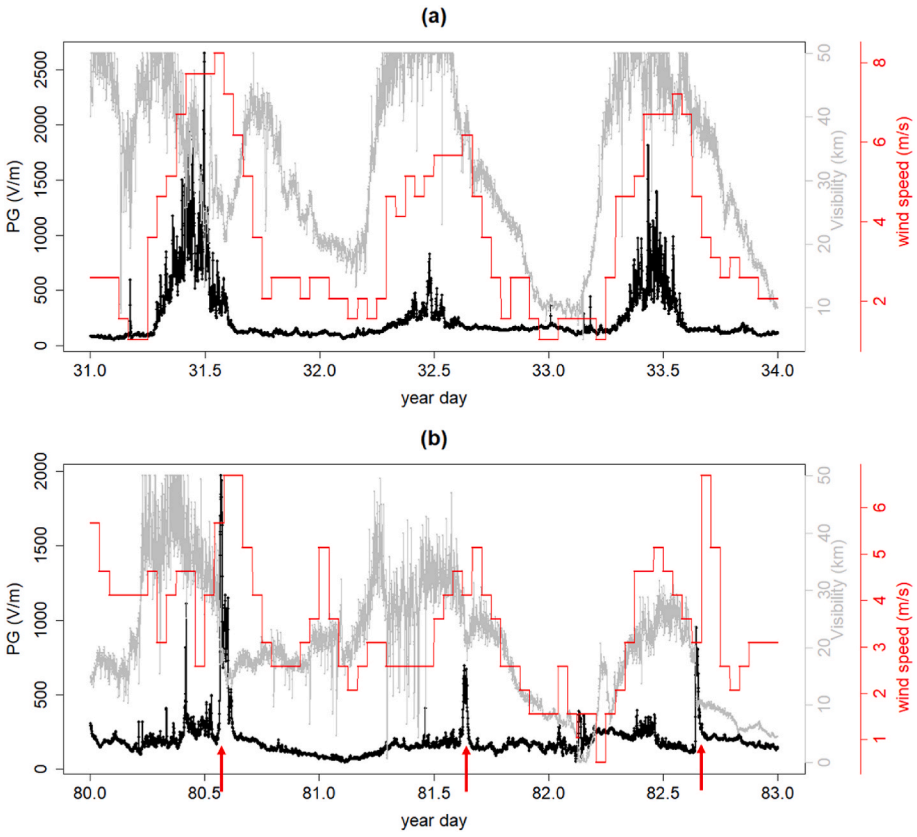

Fig. 5. Time series of PG (black), wind speed (red) and visibility (grey) at Al Ain. All data is in UT and the x-axis shows day of year in 2018. (a) Is for a typical clear day in winter, from 31st Jan to Feb 2, 2018 (day 31–34), and (b) for a series of days on which a sea breeze was detected, between 21st to March 23, 2018 (day 80–83). The stepped nature of the wind speed data (at 10m) is due to METAR observations only being available approximately every 30 min. The maximum visibility detectable by the visibility sensor is 50 km. The red arrows at the base of (b) denote arrival times of the sea breeze front.

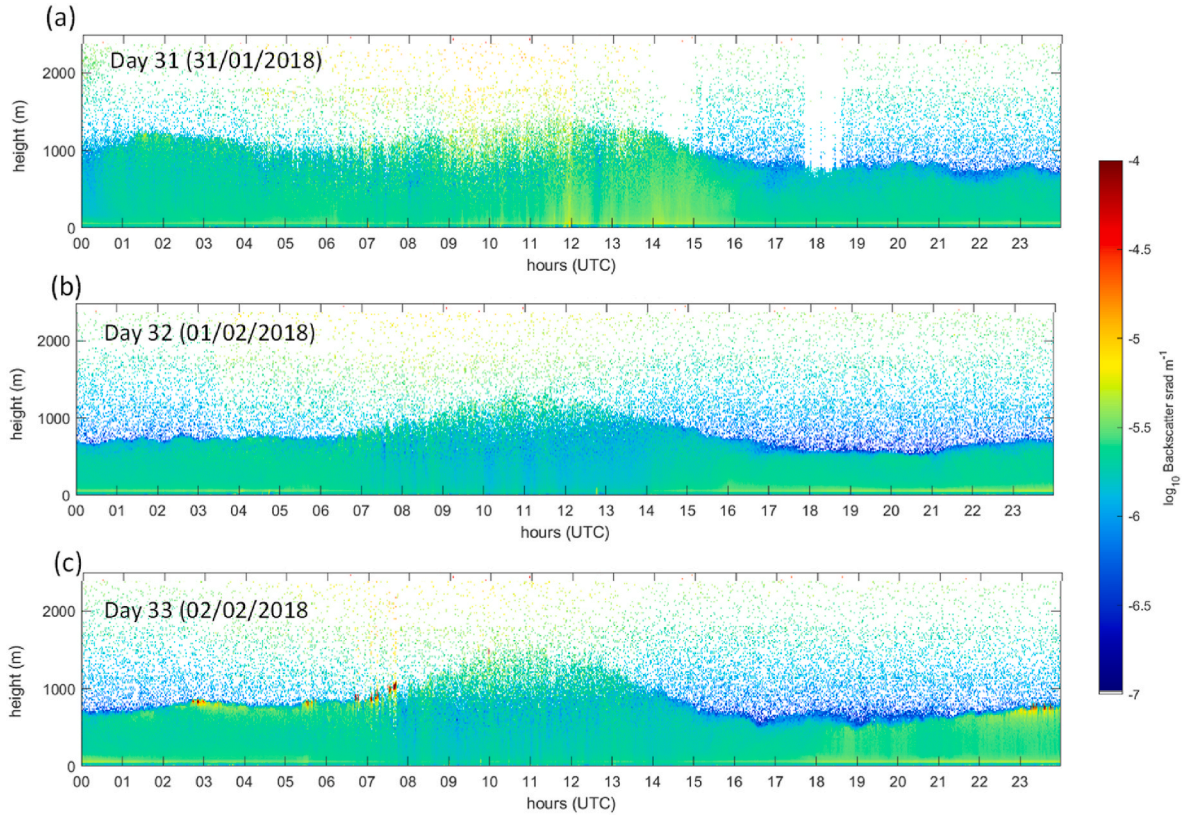

Fig. 6. Backscatter data from the CL31 ceilometer at Al Ain (data is at 20m height resolution, and 3 s time resolution) for the three convective fine days shown in Fig. 5 (a). (a) Year day 31 (January 31, 2018), (b) year day 32 (February 01, 2018) and (c) year day 33 (February 02, 2018).

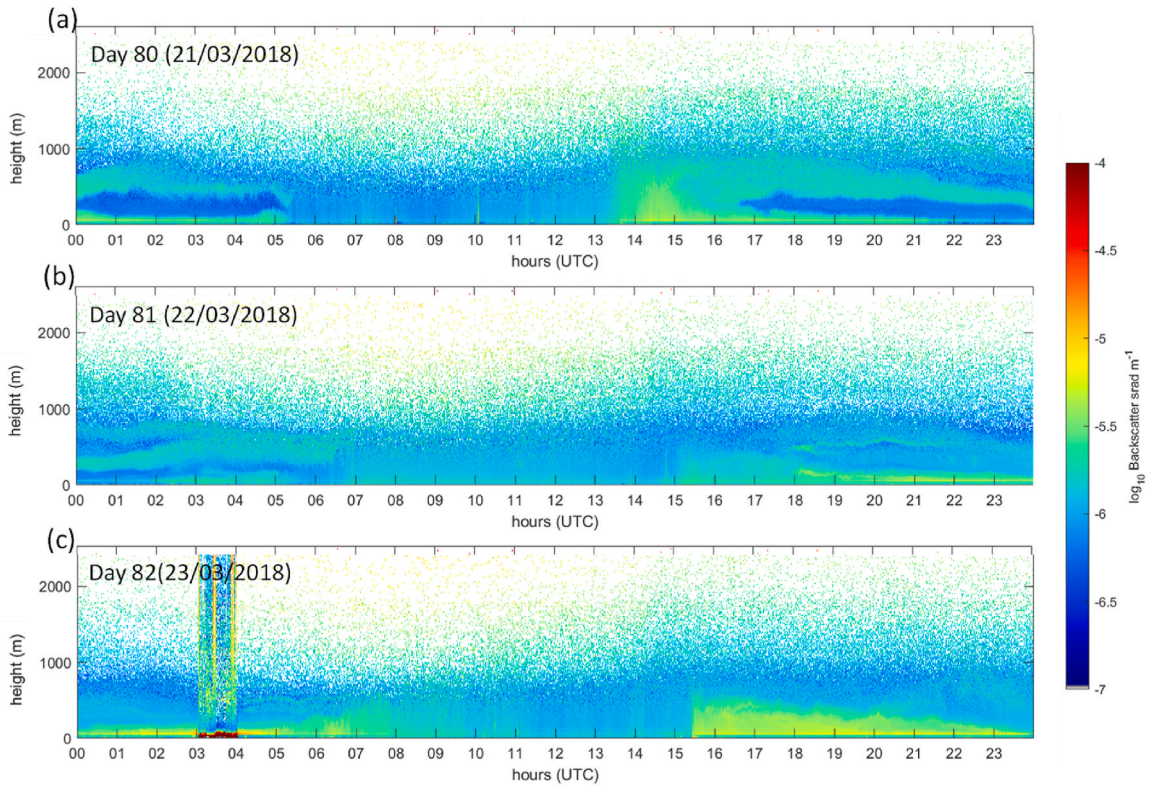

Fig. 7. Backscatter data from the CL31 ceilometer at Al Ain (data is at 20m height resolution, and 3 s time resolution) for the three sea breeze days shown in Fig. 5(b). (a) Year day 80 (March 21, 2018), (b) year day 81 (March 22, 2018) and (c) year day 82 (March 23, 2018).

3.4. Selection criteria for PG at Al Ain

Traditional meteorological criteria used in other studies for selection of fair weather PG data have had recently suggested extensions for automated sites (Harrison and Nicoll, 2018). These are typically based on conditions at mid-latitude, grass covered sites in temperate climates, with low aerosol loading, although the criteria were expected to allow for effects of snow, and resuspension of dust. Here we investigate whether these meteorological criteria can be applied to the Al Ain PG dataset to select PG values in which the local meteorological disturbance effects are minimised.

Fig. 8 shows boxplots of the PG data selected according to Harrison and Nicoll (2018) for fair weather conditions (referred to here as S1). This includes visibility >2 km, wind speed between 1 and 8 m/s, and no hydrometeors, aerosol or haze (i.e. present weather condition = 0). The median of the distribution is 112 V/m (as summarised in Table 1). Although 85% of the measured PG data values at Al Ain were obtained under these conditions, the PG range is very different (−7.7 kV/m to +13 kV/m) to those expected in fair weather conditions. This is likely due to the presence of significant ultrafine aerosol concentrations at Al Ain, which is not present at temperate, mid latitude sites. A set of revised criteria for fair weather is therefore needed for arid sites such as Al Ain, which we investigate in this section.

Bringing together the results from Figs. 5–7, it is clear that the wind and visibility criteria for a desert site are likely to differ from the conventional values summarised by Harrison and Nicoll (2018). This is primarily due to much greater aerosol loading at desert sites, with the wind affecting visibility and PG through lofting of particles. There are

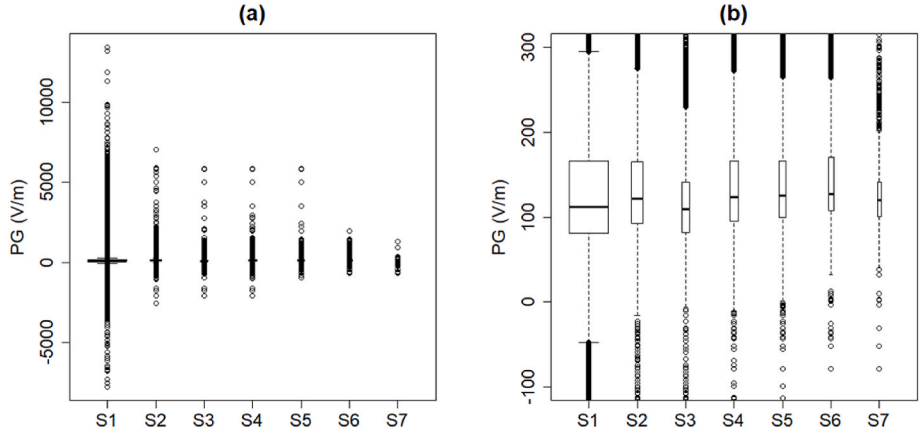

Fig. 8. (a) Boxplots of 1 min Al Ain PG values during different selection criteria (as described in Table 1). (b) Close-up of (a) between −100 and 300 V/m. The solid black line denotes the median, and dashed lines the interquartile range. The width of each box plot is proportional to the number of data points.

Table 1
Summary of various meteorological criteria applied to the Al Ain PG dataset to investigate fair weather criteria. S1 is from Harrison and Nicoll (2018).

	Selection criteria applied	Median PG (V/m)	PG range (V/m)	Number of PG values
S1	Present weather = 0, visibility >2 km, $1< U_{10} < 8$ m/s	112	−7700 to 13,400	455,929
S2	Present weather = 0, visibility >25 km, $1< U_{10} < 5$ m/s	121	−2500 to 7000	60079
S3	Present weather = 0, visibility >25 km, $1< U_{10} < 3$ m/s	109	−2100 to 5900	25,867
S4	Present weather = 0, visibility >30 km, $1< U_{10} < 5$ m/s	124	−2100 to 5900	47,368
S5	Present weather = 0, visibility >35 km, $1< U_{10} < 5$ m/s	125	−1000 to 5900	39,570
S6	Present weather = 0, visibility >40 km, $1< U_{10} < 5$ m/s	127	−700 to 2000	34,925
S7	Present weather = 0, visibility >40 km, $1< U_{10} < 3$ m/s	120	−700 to 1300	15576

typically two physical mechanisms by which aerosol can affect PG measurements: 1) through attachment of aerosol particles to ions, thereby reducing the conductivity, increasing PG; and 2) transport of charged aerosol particles (e.g. through lofting and triboelectric charging), which can cause bipolar changes in PG depending on the polarity of the aerosol charge. To investigate the influence of wind speed and visibility on PG, Fig. 9 examines the relationship between (a) PG and wind speed and (b) PG and visibility, using all PG data values from Al Ain. A clear relationship is seen between PG and wind speed, which is strongest for the larger wind speed values above 5–6 m/s (and related to dust lofting). From Fig. 9(b) it is seen that large PG values (greater than 2000 V/m) only occur at visibilities less than 25 km. Colouring the points in Fig. 9(b) according to wind speed demonstrates that most of the high visibility (>25 km) values are for wind speeds <8 m/s, and that the highest visibilities and lowest PG values are for wind speeds < 5 m/s (red points). This suggests that more appropriate selection criteria for Al Ain would be:

1. Present weather code = "No significant weather";
2. Visibility >25 km (to remove substantial dust events, mist, fog or haze from the data);
3. Wind speed between 1 and 5 m/s (to avoid dust uplift).

These new selection criteria (denoted as S2) have been applied to the Al Ain PG and the resulting data plotted as a boxplot in Fig. 8 (S2). As is summarised in Table 1, the range of PG values using S2 is still large (from −2500 to 7000 V/m) and very different from those values obtained in oceanic air or at a clean continental site. To investigate this further, "stricter" meteorological criteria (in the sense of selecting quiescent days meteorologically) are applied to the Al Ain PG, as summarised in Table 1, and plotted in Fig. 8. Fig. 8 shows that the range of PG values is not substantially reduced until S6 and S7, which is when visibility >40 km. A consequence from increasing the strictness of meteorological criteria in that the number of PG values decreases from 60079 for S2 to 15576 for S7 (as shown in Table 1).

To determine the most suitable selection criteria for Al Ain, whilst maintaining a reasonable number of data points to analyse, we now investigate the robustness of the diurnal cycle in PG for the various different selection criteria considered.

4. Diurnal variation in PG

4.1. Fair weather diurnal variation

This section investigates the typical diurnal variation in PG observed at Al Ain for the different selection criteria in Table 1, in order to understand the sources of variability present at Al Ain. Fig. 10(a) shows the hourly median diurnal variation in PG at Al Ain for all weather conditions. This demonstrates a single sharp maximum at 14UT (18LT), with median values up to 250 V/m at the peak, this gradually decreases during the late afternoon and returns to more fair weather values (around 100 V/m) during the local evening and night periods. The time of the maximum is likely related to local sources of variability, specifically the sea breeze, as discussed in section 3.3.2.

To examine the robustness of the diurnal cycle in PG for the various meteorological selection criteria in Table 1, Fig. 10(b) shows PG selected according to S1–S7. These all show a single maximum, but the time of this peak is different for S1 (based on Harrison and Nicoll, 2018), than for the other criteria. For S1 the peak occurs around 14UT, which is the same for "all conditions" as in Fig. 10(a), and is likely caused by the sea breeze. The time of the peak in the diurnal variation in PG for S2 – S7 is shifted to much earlier times at 07UT (11LT), and the maximum PG

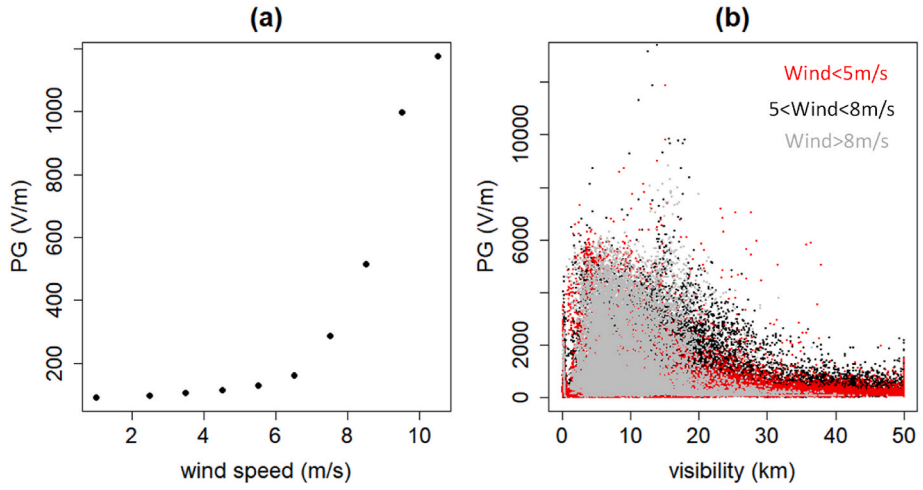

Fig. 9. Relationship between (a) PG and wind speed, and (b) PG and visibility. PG data in (a) are binned together according to wind speed (with 1 m/s bins, except for the lowest wind speed (<2 m/s)). 1 min PG and visibility is plotted in (b) and coloured according to wind speed (red = wind speed < 5 m/s, black = wind speed between 5 and 8 m/s, grey = wind speed >8 m/s).

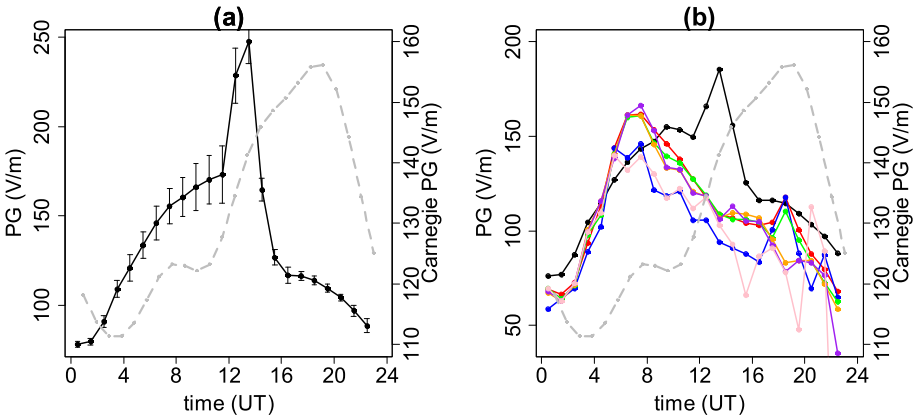

Fig. 10. Diurnal variation in Al Ain PG for (a) all conditions, and (b) selected low disturbance conditions (defined according to Table 1. Colours are: S1 = black, S2 = red, S3 = blue, S4 = green, S5 = orange, S6 = purple, S7 = pink). The left-hand PG axis in (b) is restricted from 50 to 200 V/m. Data points are hourly medians (from 1 min values), and error bars are 2 standard errors on the mean. The grey dashed points are the PG from the Carnegie vessel (Harrison, 2013).

value is much lower at 160 V/m. This peak is again likely related to local processes, including convection, which we explore in the following section. There is also a hint of a small secondary maximum at 17UT (21LT), which roughly coincides with the main peak of the Carnegie variation (at 19UT), but may be more likely related to land breeze effects which can occur after sunset. To investigate this further we examined the diurnal variation in PG for criteria S2 for wind directions independent of the land breeze, which tends to blow from the south-east. The 17UT peak is still present, which suggests the possibility of a GEC influence, but this is not a robust conclusion as the maxima is only a single point. The shape and magnitude of the median diurnal variation is similar for S2–S7, which suggests that the diurnal PG cycle is fairly independent of the exact choice of selection criteria. In order to maximise the number of available data points, we apply selection criteria S2 for further analysis of the PG data in this paper.

4.2. Seasonal differences in diurnal variation in PG

To examine the convective influences on the diurnal PG variation at Al Ain, the data can be split into two main seasons: March to November where convection is substantial; and November to March, which is the winter season where convection is much less, but still present (as shown in Fig. 5). Fig. 11(a) shows the diurnal curves for these two seasons for PG during all weather conditions. Both seasons show a single daily maximum in PG, with the magnitude of the PG values being much larger in the convective season (up to 350 V/m) than the winter season (up to 150 V/m). The timing of the maximum is also different, with the winter maxima occurring much earlier (07UT) than the convective maxima (14UT). The convective peak is also much sharper than the winter peak. This may be related to different physical processes being responsible for the PG peak – with the sea breeze dominating during the convective season, and more general convection processes dominating during the winter season.

The seasonal diurnal variation can be further examined by selecting PG values (according to S2 in Table 1), which is shown in Fig. 11(b). Again, the magnitude of the PG values differs between the seasons, with larger PG values during the convective months. The timing of the single maximum is consistent between the seasons, (and also with the winter curve in Fig. 11 (a)) which suggests that it is the same physical process that drives the diurnal variation in both seasons (i.e. tropical convection) and that the effect of the sea breeze has been removed by the selection criteria. The sharp minimum at 15UT in the convective months should not be considered robust, as the number of data points around this time is much less than at other times of the day (i.e. 107 vs 1528 data points at the time of the maximum at 09UT).

4.3. Diurnal variation in meteorological parameters

Fig. 12 examines how the diurnal variations in wind speed, visibility and temperature relate to the diurnal variation in PG (for the whole year), plotted in local time (which is different from the other figures). Fig. 12(a), (c) and (e) show data for PG, wind speed, visibility and

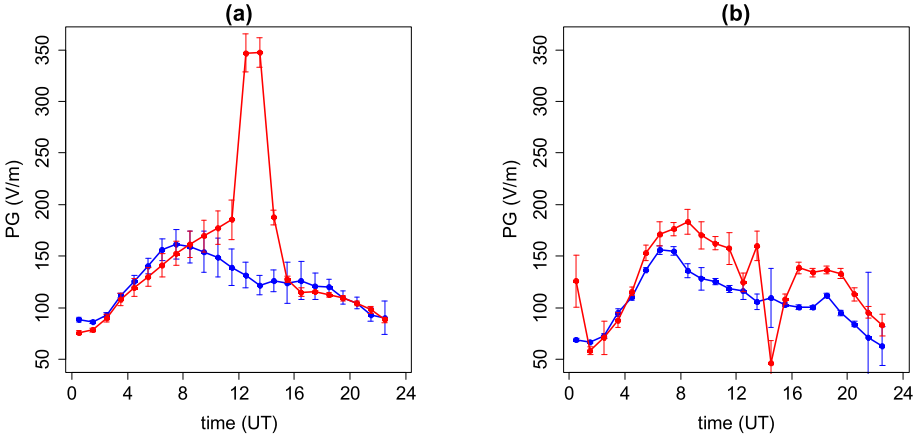

Fig. 11. Seasonal diurnal variation in Al Ain PG for (a) all conditions, and (b) low disturbance conditions (as defined according to S2 in Table 1). Seasons are grouped into March–November (red), which is the "convective" season, and November–March (blue) "winter" season. Error bars given represent 2 standard errors on the mean.

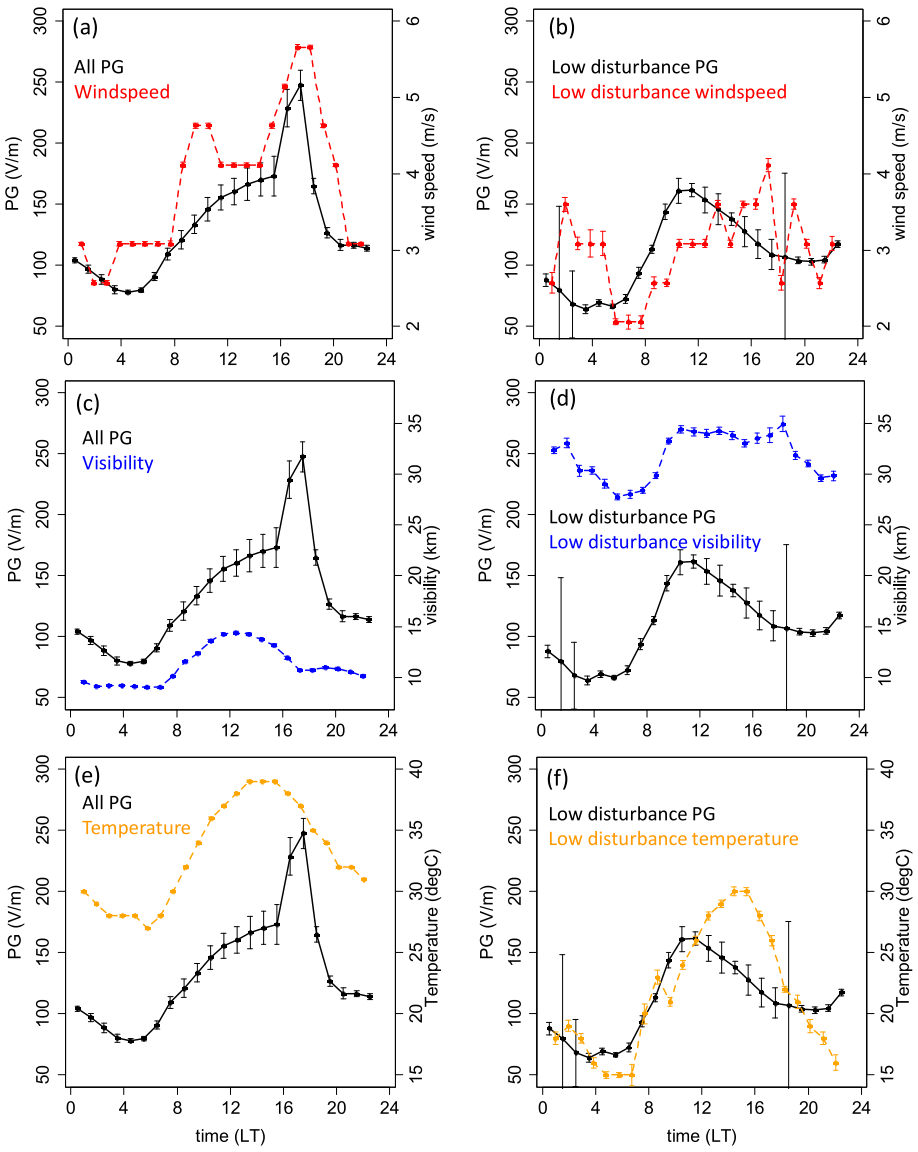

Fig. 12. Diurnal variation in PG during all conditions ((a), (c) and (e)) and low disturbance conditions ((b), (d) and (f)) ((defined according to S2 in Table 1). Hourly median in 10m wind speed is shown in red, visibility in blue, and temperature in orange for all conditions ((a),(c) and (e)), and for time periods corresponding to S2 selected PG values only ((b), (d), (f)). Data points are hourly medians (based on 1 min values) and error bars are 2 standard errors on the mean. N.B. data is plotted in local time (LT), unlike in the other plots.

temperature in all weather conditions. The wind speed increases throughout the day, with multiple peaks: at 09LT - presumably related to convective processes arising due to sunrise - and a main peak at 18LT, before decreasing during the evening hours. The shape of this variation is very similar to the variation in PG, with the main maxima of the two curves occurring within an hour of each other (likely related to sea breeze activity). The visibility variation for all conditions (Fig. 12(c)) shows minimum values nocturnally, and starts to increase after sunrise (typically 0530-0700LT) as convective mixing begins. It continues to increase until 12LT, then decreases during the afternoon and into evening, likely related to increasing amounts of dust and aerosol pollution due to daytime anthropogenic activity and sea breeze circulations. From Fig. 12 (e), the daily variation in temperature shows a maximum around 14LT, which is before the maximum in PG and wind speed. The PG peak at 18LT therefore occurs at a time of relatively reduced visibility, and at the same time as the maximum in wind speed, which is consistent with what we would expect from sea breeze effects.

Fig. 12 (b), (d) and (f) show the diurnal variation in low disturbance PG, wind speed, visibility and temperature during periods of low disturbance PG (defined according to S2 in Table 1). It should be noted that the wind speed during these periods is much reduced, the visibility greater, and the temperatures less than in the plots for All Conditions. The shape of the diurnal variation in wind speed is quite different to All Conditions, during the low disturbance periods, with a very early morning peak around 4LT which may be linked to nocturnal jet activity within the BL. There is also no sunrise peak in wind speed in low disturbance conditions. Although the main peak in wind speed occurs around (17LT) (which is the same as during All Conditions), this no longer coincides with the maxima in low disturbance PG (which occurs much earlier at 10LT). Fig. 12(d) shows that the variation in low disturbance visibility has a minimum in the early morning hours, and increases following sunrise, but with a much broader peak than the low disturbance PG curve. The increase in visibility following sunrise takes place on the same timescale as the morning increase in PG. This suggests that the aerosols responsible for the PG and visibility changes are being controlled by the same mixing processes (through transport of space charge). It should be noted that the high visibility values around this time (36 km) suggest that the air is actually relatively "clean" in terms at least of micron-sized dust particles, and certainly in comparison to the All Conditions case.

5. Discussion

The aim of this study is to characterise the influences on the PG at Al

Ain. It is clear from the analysis presented here that convective processes are the main factor controlling the PG at Al Ain. The diurnal variations shown in Figs. 10–12 demonstrate that without any selection for fair weather conditions, the median hourly values of PG reach 250 V/m (with mean values up to 800 V/m), with a single maximum around 14UT (18LT). This maximum coincides with the daily maximum in wind speed, and a period of low visibility conditions. These features, as well as the sharp nature of this peak, makes it highly likely that it is the regular sea breeze circulation (which is present on 77% of days (Eager et al., 2008) which dominates the diurnal variation in PG most of the time. When seasonal variations are considered, the magnitude of the PG peak in winter is much lower (150 V/m compared to 350 V/m) than during convective summer conditions, and the time of the maxima is also shifted to earlier times. This indicates that the sea breeze effect primarily dominates during the summer, as also found by Eager et al. (2008).

To study potential GEC influences on the PG, only electrically undisturbed conditions should be analysed. Even though 95% of the time, the present weather code at Al Ain is classified as "no significant weather", this clearly does not correspond to "electrically fair weather" conditions. Section 3.4 demonstrates that the criteria typically used to define fair weather at other sites (e.g. as summarised by Harrison and Nicoll, 2018) are not sufficient to remove local influences at Al Ain. The analysis in section 3.4 demonstrates that reducing the upper limit on the usual FW wind speed (from 8 to 5 m/s) and increasing the visibility criteria (from >2 to >25 km) helps to reduce the effect of local aerosol on the PG at Al Ain, but not completely. A summary of the "traditional" FW criteria and the new criteria defined here for Al Ain is given in Table 2. The resulting low disturbance diurnal variation in PG shows a single maximum, but this occurs at 07UT (11LT), rather than the 19UT maximum of the Carnegie curve. This suggests that the main influence on the Al Ain PG diurnal variation is local, rather than global. Although surface radioactivity measurements, aerosol particle size and concentration, as well as aerosol mineralogy measurements would have been beneficial in further understanding the details of the diurnal variation curve, these were not available during the campaign. Unlike at other sites, where a Carnegie-like variation may be present during certain seasons, at Al Ain, even the winter season shows evidence of substantial convective mixing, which dominates the selected PG values.

6. Conclusion

This paper presents detailed analysis of a new atmospheric electricity data set to measure PG in the United Arab Emirates. PG measurements in arid, desert environments such as this are rare, and can provide insight into convective and aerosol transport processes. In this work we examined the factors influencing the PG at Al Ain, and demonstrated that this site is highly dominated by local convective process and sea breeze circulations. The diurnal variation in PG during all weather conditions showed a single maximum at 14UT (18LT), which corresponds with the maxima in wind speed, and low visibility values. Such conditions are known to be associated with the arrival of the sea breeze front at Al Ain, which occurs throughout the year, and clearly dominates the behaviour of the PG. By considering the effects of wind speed and visibility on PG we define criteria for fair weather conditions (including wind speed between 1 and 5 m/s and visibility >25 km), which remove the sea breeze effect on the PG, but still highlight the dominance of local convective processes on the PG at Al Ain. The influence of convection on PG is evident even during the winter months when convection is much more suppressed than during the summer. All of these fair weather conditions also coincide with present weather sensor reports of "no significant weather" (which is the dominant weather condition at Al Ain for 95% of the time). The prevalence of high aerosol loading, and year round convective processes means that the environment at Al Ain is significantly electrified most of the time during daylight hours. This suggests that dusty sites such as Al Ain are not suitable for studying global influences on atmospheric electricity, but are well suited for research into dust charging and convective processes. The regularly observed large PG values (of kV/m) and high PG variability (particularly during the summer months) indicates the prevalence and abundance of charged dust, which has implications for dust lofting processes, satellite remote sensing of dust particles, as well as long range transport of elevated dust layers and preferential scavenging of charged dust by water droplets.

Table 2
Summary of existing meteorological criteria from Harrison and Nicoll (2018) for fair weather conditions at temperate climate sites, and proposed new selection conditions for arid sites (S2 from Table 1).

Meteorological parameter affecting the PG	Existing FW criteria	Suggested selection criteria for arid sites
Aerosol	No hydrometeors of any kind, i.e. visibility >2 km	Visibility >25 km (to further minimise aerosol effects)
Cloud	No low stratus cloud, fog or convective cloud	Present weather condition = 0 (i.e. no significant weather)
Wind speed	U_{10} wind speed between 1 and 8 m/s	U_{10} wind speed between 1 and 5 m/s to minimise aerosol lofting and resuspension

Declaration of competing interest

The authors declare that they have no known competing financial interests or personal relationships that could have appeared to influence the work reported in this paper.

Data availability

Potential Gradient and Visibility data are openly available and can be obtained from the University of Reading Data Repository at https://doi.org/10.17864/1947.000362. METAR data were obtained from https://mesonet.agron.iastate.edu/request/download.phtml?network=AE_ASOS.

Acknowledgements

This material is based on work supported by the National Center of Meteorology, Abu Dhabi, UAE under the UAE Research Program for Rain Enhancement Science. KAN acknowledges a NERC Independent Research Fellowship (NE/L011514/1) and (NE/L011514/2). AAK acknowledges a studentship from the Scholarship Coordination Office (SCO), Abu Dhabi, UAE. Martin Airey and Graeme Marlton contributed to the measurements and data acquisition.

References

Abuelgasim, A., Farahat, A., 2020. Effect of dust loadings, meteorological conditions, and local emissions on aerosol mixing and loading variability over highly urbanized semiarid countries: United Arab Emirates case study. J. Atmos. Sol. Terr. Phys. 199, 105215.

Awad, M.M., Said, H.M., Arafa, B.A., Sadeek, A.E.H., 2002. Effect of sandstorms with charged particles on the flashover and breakdown of transmission lines. In: Proc. 2002 International Council on Large Electric Systems Conf, pp. 306–309.

Bagnold, R.A., 1941. *The Physics of blown Sand and desert dunes* (chelmsford, MA: courier corporation (cited in Zheng X J 2013 electrification of wind-blown sand: recent advances and key issues. *Eur. Phys. J.* E 36, 1–15).

Branch, O., Behrendt, A., Gong, Z., Schwitalla, T., Wulfmeyer, V., 2020. Convection initiation over the eastern arabian peninsula. Meteorol. Z. 29 (1), 67–77. https://doi.org/10.1127/metz/2019/0997.

Bennett, A.J., Harrison, R.G., 2007. Atmospheric electricity in different weather conditions. Weather 62 (10), 277–283.

Eager, R.E., Raman, S., Wootten, A., Westphal, D.L., Reid, J.S., Al Mandoos, A., 2008. A climatological study of the sea and land breezes in the Arabian Gulf region. J. Geophys. Res. Atmos. 113 (D15).

Esposito, Francesca, et al., 2016. The role of the atmospheric electric field in the dust-lifting process. Geophys. Res. Lett. 10, 5501–5508.

Filioglou, M., Giannakaki, E., Backman, J., Kesti, J., Hirsikko, A., Engelmann, R., O'Connor, E., Leskinen, J.T.T., Shang, X.X., Korhonen, H., Lihavainen, H.,

Romakkaniemi, S., Komppula, M., 2020. Optical and geometrical aerosol particle properties over the United Arab Emirates. Atmos. Chem. Phys. 20 (14), 8909–8922. https://doi.org/10.5194/acp-20-8909-2020.
Harris, D.J., 1967. Electrical effects of the Harmattan dust storms. Nature 214 (5088), 585-585.
Harrison, R.G., 2013. The carnegie curve. Surv. Geophys. 34 (2), 209–232.
Harrison, R.G., 2020. Behind the curve: a comparison of historical sources for the Carnegie curve of the global atmospheric electric circuit. History. Geo. Space Sci. 11 (2), 207–213.
Harrison, R.G., Nicoll, K.A., 2018. Fair weather criteria for atmospheric electricity measurements. J. Atmos. Sol. Terr. Phys. 179, 239–250.
Kamra, A.K., 1972. Measurements of the electrical properties of dust storms. J. Geophys. Res. 77 (30), 5856–5869.
Katz, S., Yair, Y., Price, C., Yaniv, R., Silber, I., Lynn, B., Ziv, B., 2018. Electrical properties of the 8–12th September, 2015 massive dust outbreak over the Levant. Atmos. Res. 201, 218–225.
Kurosaki, Y., Mikami, M., 2007. Threshold wind speed for dust emission in east Asia and its seasonal variations. J. Geophys. Res. Atmos. 112, D17.
Nicoll, K.A., Harrison, R.G., Ulanowski, Z., 2011. Observations of Saharan dust layer electrification. Environ. Res. Lett. 6, 014001. http://stacks.iop.org/1748-9326/6/014001.
Nicoll, K.A., Harrison, R.G., Barta, V., Bor, J., Brugge, R., Chillingarian, A., et al., 2019. A global atmospheric electricity monitoring network for climate and geophysical research. J. Atmos. Sol. Terr. Phys. 184, 18–29.
Nicoll, K., Harrison, G., Marlton, G., Airey, M., 2020. Consistent dust electrification from Arabian Gulf sea breezes. Environ. Res. Lett. 15 (8), 084050.
Rudge, W.D., 1913. Atmospheric electrification during South African dust storms. Nature 91 (2263), 31–32.
Rycroft, M.J., Harrison, R.G., Nicoll, K.A., Mareev, E.A., 2008. An overview of Earth's global electric circuit and atmospheric conductivity. Atmos. Electr. 83–105.
Semeniuk, T.A., Bruintjes, R., Salazar, V., Breed, D., Jensen, T., Buseck, P.R., 2015. Processing of aerosol particles within the Habshan pollution plume. J. Geophys. Res. Atmos. 120 (5), 1996–2012.
Ulanowski, Z., Bailey, J., Lucas, P.W., Hough, J.H., Hirst, E., 2007. Alignment of Atmospheric Mineral Dust Due to Electric Field.
Van der Does, M., Knippertz, P., Zschenderlein, P., Harrison, R.G., Stuut, J.B.W., 2018. The mysterious long-range transport of giant mineral dust particles. Sci. Adv. 4 (12), eaau2768.
Wehbe, Y., Ghebreyesus, D., Temimi, M., Milewski, A., Al Mandous, A., 2017. Assessment of the consistency among global precipitation products over the United Arab Emirates. J. Hydrol.: Reg. Stud. 12, 122–135. https://doi.org/10.1016/j.ejrh.2017.05.002.
Wehbe, Y., Tessendorf, S.A., Weeks, C., Bruintjes, R., Xue, L., Rasmussen, R., Lawson, P., Woods, S., Temimi, M., 2021. Analysis of aerosol–cloud interactions and their implications for precipitation formation using aircraft observations over the United Arab Emirates. Atmos. Chem. Phys. 21 (16), 12543–12560.
Whipple, F.J.W., 1929. On the association of the diurnal variation of electric potential gradient in fine weather with the distribution of thunderstorms over the globe. Q. J. R. Meteorol. Soc. 55 (229), 1–18.
Whipple, F.J.W., Scrase, F.J., 1936. *Point Discharge in the Electric Field of the Earth, an Analysis of Continuous Records Obtained at Kew Observatory* (No. 68). HM Stationery Office.
Williams, E., Nathou, N., Hicks, E., Pontikis, C., Russell, B., Miller, M., Bartholomew, M. J., 2009. The electrification of dust-lofting gust fronts ('haboobs') in the Sahel. Atmos. Res. 91 (2–4), 292–298.
Wilson, C.T.R., 1921. III. Investigations on lighting discharges and on the electric field of thunderstorms. Philos. Trans. R. Soc. Lond. - Ser. A Contain. Pap. a Math. or Phys. Character 221 (582–593), 73–115.
Yair, Y., Katz, S., Yaniv, R., Ziv, B., Price, C., 2016. An electrified dust storm over the Negev desert, Israel. Atmos. Res. 181, 63–71.
Yaniv, R., Yair, Y., Price, C., Katz, S., 2016. Local and global impacts on the fair-weather electric field in Israel. Atmos. Res. 172, 119–125.
Yousef, L.A., Temimi, M., Wehbe, Y., Al Mandous, A., 2019. Total cloud cover climatology over the United Arab Emirates. Atmos. Sci. Lett. 20, 2. https://doi.org/10.1002/asl.883.
Zhang, H., Zhou, Y.H., 2020. Reconstructing the electrical structure of dust storms from locally observed electric field data. Nat. Commun. 11 (1), 1–12.
Zheng, X.J., 2013. Electrification of wind-blown sand: recent advances and key issues. European Phy. J. E. 36 (12), 1–15.
Zhou, Y.H., He, Q.S., Zheng, X.J., 2005. Attenuation of electromagnetic wave propagation in sandstorms incorporating charged sand particles. European Phy. J. E. 17 (2), 181–187.